

Seismic behaviour of a three-story half scale confined masonry structure

A.San Bartolomé, D.Quiun & D.Torrealva
Catholic University, Peru

ABSTRACT: The objective of this research was the analytical and experimental study (shaking table test) on the seismic behaviour of a reduced scale model (1:2.5), whose walls represent one perimetric wall of a 3-story building, made of clay masonry confined by reinforced concrete elements. The vibration properties, strength of materials and axial stress of the model were similar to those of actual buildings. In addition, the study included a previous static test on the specimen; in which the elastic behaviour was investigated. The results of both tests were used to revise the actual criteria on analysis and design of confined masonry buildings.

1 SPECIMEN CHARACTERISTICS

The geometry of the specimen is given in Figure 1. The strength of materials, axial stress, damping and the vibration period were similar to those of actual 3-story confined masonry buildings; to achieve this, reinforced concrete slabs with added load and similar materials were used in the model. Under such considerations, the seismic excitation was not scaled.

The specimen weight was 57.78 kN; therefore, the axial stress in the first-story walls was 0.33 MPa.

1.1 Material properties

The materials used in the construction of the specimen had the followings properties:

1. The masonry units were solid clay bricks, with original dimensions 240x135x70 mm and 11 MPa compressive strength. This unit was cut in three parts which were laid using the original brick surface.
2. The mortar used was 1:4 (portland cement: sand) by volume, having a compressive strength of 6 MPa; the mortar joint thickness was 5 mm.
3. The concrete used in the columns was a coarse aggregate grout (slump 200 mm), with compressive strength $f'_c = 15$ MPa and elastic modulus $E_c = 13700$ MPa.
4. Four masonry prisms with dimensions 75x135x375 mm (5 layers) were tested to axial compression, the strength was $f'_m = 6$ MPa and the elastic modulus was $E = 1510$ MPa.
5. Four square masonry prisms with dimen-

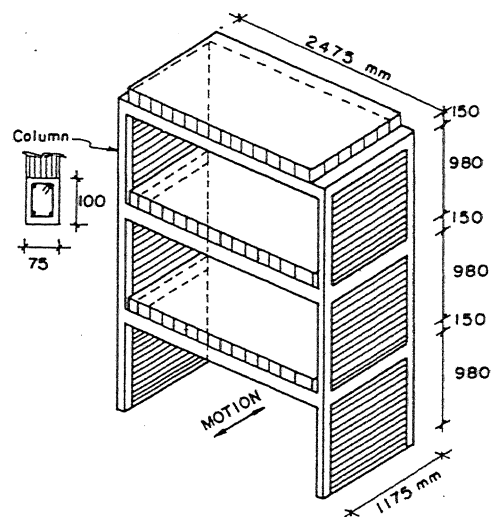


Fig. 1 Geometry of the 3-story confined masonry specimen

sions 75x375x375 mm (5 layers) were tested to diagonal compression, giving a shear strength $v'_m = 0.8$ MPa and a shear modulus $G = 450$ MPa.

6. The vertical reinforcement in each column was 4-#5.5 mm wire steel. The yield stress was 220 MPa and the ultimate stress was 316 MPa; the stress-strain relationship had yield plateau and strain hardening similar to a normal steel.



Fig. 2 Static test to evaluate $[f]$

Table 1. Assumed force distribution in one specimen's wall

Story	Height h(mm)	Lat. Force	Shear V	Moment M	Axial P(kN)
3	1130	3F	3F	3Fh	9.63
2	1130	2F	5F	8Fh	19.26
1	1130	F	6F	14Fh	28.89

2 SPECIMEN DESIGN AND STRENGTH CAPACITY

2.1 Design

The specimen was designed according to the Peruvian Code (ININVI 1982). The seismic coefficient, reduced by ductility, was $c = 0.16$. The calculated reinforcement in each column was 2-#5.5, but 4-#5.5 were used because the minimum number of bars is 4.

Another goal of this research was to see whether horizontal reinforcement worked under dynamic conditions, so in the first-story walls a small ratio of 0.016% was used (1-#1.8 every 3 layers anchored in the columns). It must be mentioned that in Peru it is not common to use horizontal reinforcement in confined masonry walls.

2.2 Flexural capacity

The flexural capacity of each wall was evaluated in terms of the first-story shear force associated to the yielding and to the ultimate stress of the actual vertical reinforcement. For this evaluation, a triangular lateral force distribution was assumed as shown in Table 1. Equating the external moment (including the axial load effects) to the internal resisting moment, shear forces of 15 kN and 19 kN were obtained for yielding and ultimate stress of the reinforcement, respectively.

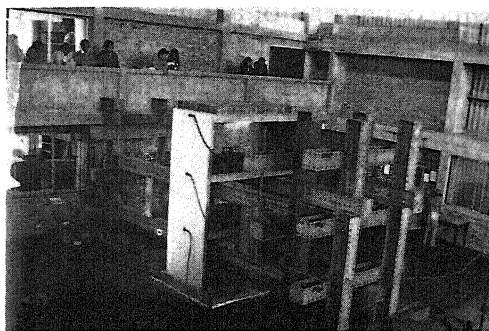


Fig. 3 Shaking table test

2.3 Shear capacity (VR)

The shear capacity of each wall (VR) was evaluated using formula 1 (San Bartolomé 1990). Using the triangular lateral force distribution, the value $VR = 22$ kN was obtained for the first-story walls; this result is greater than the values associated to the yielding flexural capacity (15 kN) and also to the maximum flexural capacity (19 kN). Therefore, a flexural failure was expected.

$$VR = (0.5 v'm \alpha + 0.23 \sigma) A \quad (1)$$

in which:

$v'm = 0.8 \text{ MPa}$ (see item 1.1.5)

$A =$ gross section area $= t L$

$t =$ wall thickness $= 75$ mm

$L =$ wall length $= 1175$ mm

$\sigma =$ axial stress $= P/A$

$\alpha =$ slenderness reduction factor:

$$1/3 < \alpha = V L/M < 1$$

$P, V, M =$ axial load, shear force and bending moment (see Table 1)

3 CALCULATION OF THE FLEXIBILITY MATRIX $[f]$ AND NATURAL PERIOD (T)

3.1 Experimental and analytical evaluation of the flexibility matrix $[f]$ in the elastic range

The experimental evaluation of $[f]$ was performed subjecting the specimen to a lateral increasing load, applied independently in each of the specimen's three floors (Figure 2); the lateral displacements were measured with LVDT.

For the analytical calculation of $[f]$, the experimental results obtained on the prisms (E, Ec, G) and two different approaches were used:

1. Plane frame. One wall was modeled as a

Table 2. Flexibility Matrix $[f] \times 10^{-2}$ mm, for a lateral load of 2.5 kN in each wall (5 kN in the specimen)

Plane Frame	Fin. elem.	Experimental
9 12 14	7 9 12	7 11 17
12 28 39	9 23 33	11 27 41
14 39 69	12 33 58	17 41 71

Table 3. Shaking table test runs

Run	D (mm)	Platform Accel. (g)
A	15	0.14
B	50	0.52
C	80	0.85

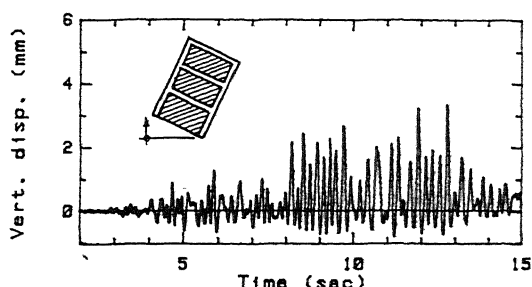


Fig. 4 Vertical displacement at the wall base end in run B

cantilever beam with flexural and shear deformations; the cross section (concrete-masonry) moment of inertia was obtained using the transformed section criteria.

2. Finite element. Four-node plane rectangular elements with two translational degrees of freedom per node were used.

The matrix $[f]$ coefficients appear in Table 2, in which it may be observed that the differences between the analytical and experimental results are small. Therefore, a plane frame analysis is adequate to predict the elastic behaviour of confined masonry structures.

3.2 Experimental and analytical evaluation of natural period T

Two experimental methods were used for free vibration test, in which the specimen response was measured using an accelerometer located at the third story. The first one consisted in hitting the specimen at each level; the second method consisted in applying small pulses at the base of the specimen once it was installed on the shaking table (Figure 3).

For the analytical evaluation of T, the specimen was modeled as a lumped mass system, using the different matrices $[f]$ previously

determined and the Jacobi method.

The analytical and the experimental T values in seconds for the first vibration mode were as follows:

1. $[f]$ experimental and Jacobi: 0.12
2. $[f]$ plane frame and Jacobi: 0.12
3. $[f]$ finite elem. and Jacobi: 0.11
4. Hitting the specimen: 0.10
5. Pulses with shaking table: 0.13

4 DYNAMIC TEST

Before the dynamic test, a step-by-step inelastic analysis was performed modeling the specimen as a lumped mass system. In the elastic range, the experimental matrix $[f]$ was utilized, while in the inelastic range, a bilinear non-degrading shear force-displacement relationship in every story was assumed. The input wave was the L component of the May 31, 1970 earthquake, recorded in Lima (27 seconds). The results of these analyses were used to establish 3 runs on the shaking table; each run was preceded by a free vibration test, consisting in four pulses of small amplitude.

The horizontal excitation was in the wall's direction (Figure 1) and the peak platform displacement (D) for each run is shown in Table 3.

Six accelerometers were used to calculate the inertia forces in each wall; later, the time history of the bending moments and shear forces were calculated by equilibrium.

5 RESULTS AND COMMENTS

5.1 Behaviour of the specimen

In run A no cracking occurred. At run B a flexural crack appeared at the walls base, causing the yield of the vertical reinforcement; the walls rocking may be observed in Figure 4.

The shear failure in both first-story walls occurred in run C, at the end of the test the specimen was in an irreparable condition as shown in Figure 5. During this run the horizontal reinforcement broke (showing that it effectively worked under dynamic conditions), inducing the sliding of the upper stories across the first-story diagonal cracks.

5.2 Period of vibration T and damping ratio β

The vibrations obtained by hitting the specimen produced low values for T and β , as compared to the method of pulses on the shaking table or the analytical model using matrix $[f]$. Given the good results obtained using a plane frame analysis, such method may be used to predict T, modeling the structure as a

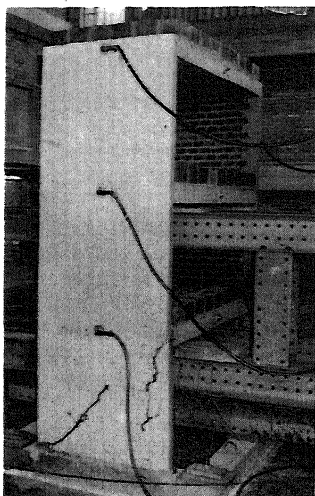


Fig. 5 Specimen after run C

lumped mass system and using $\beta = 4\%$. On the other hand, an increase in the excitation produced an increase on T and β ; so, after the base flexural crack occurred in run B, the stiffness degraded to 50% of its initial value while β remained constant at 4%, and at the end of the test (run C), the stiffness was only 11% of its initial value, while the β value increased to 7%.

5.3 First flexural crack prediction

By using the transformed section criteria and a triangular system of inertia forces, it is possible to determine the base moment that produces the first tension crack at the columns (equating the actual axial stress to the cracking strength $\approx 0.15 f'c$). In this way, a moment $M = 31.4$ kN-m was obtained at the base for one wall, while the experimental result in run B was $M = 32.9$ kN-m.

5.4 Shear strength prediction (VR)

Formula 1 was applied to evaluate $VR = 22$ kN for one wall. This prediction is 13% less than the experimental value obtained in run C (24.9 kN), so the correlation is acceptable.

5.5 Flexural failure theory

Although the final flexural failure was theoretically expected, it did not take place, and the following comments may be made:

1. The vertical reinforcement yielded during run B; however, the shear force continued increasing in run C (see Figure 6), until the specimen had a shear failure. If the final

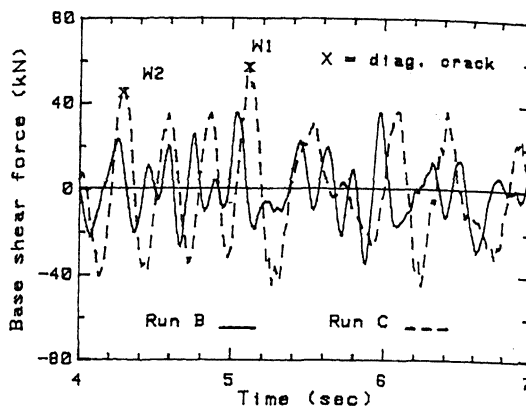


Fig. 6 Time history of the total base shear force at runs B and C

flexural failure had occurred, the damping would have increased and the shear force would have remained nearly constant, neither of which occurred.

2. The specimen satisfied several of the ideal characteristics to obtain a flexural failure: it was an slender cantilever without in-plane beams, with rectangular section (without transverse walls) and had a theoretical flexural capacity less than the shear capacity; even though, the final failure was of shear type.

One of the reasons for this behaviour is that at the time of the shear failure, the lateral force distribution changed from triangular to uniform (see Figure 7), decreasing the base moment. Another reason could be that the maximum flexural capacity might have increased, due to the vertical inertia forces generated by the specimen rocking and to the increase on the strength of the vertical reinforcement by dynamic effects (the reinforcement steel strength in item 1.1.6 was determined from a static test).

3. Specimen design according to the flexural failure theory (Priestley 1986), using a seismic coefficient reduced by ductility $c = 0.16$ (Peruvian Code), the flexural strength reduction factor and factored loads, resulted in a smaller vertical reinforcement at the columns (1-#5.5).

In the eventuality of using such reinforcement, the accumulated energy till the time of the occurrence of the shear failure could not be absorbed by the structure, and the collapse could have been produced by the fracture of the vertical reinforcement.

5.6 Shear failure design theory

This design theory uses the criteria that the columns take the diagonal cracking load and the associated axial loads due to bending moment; also, a minimum horizontal reinforcement

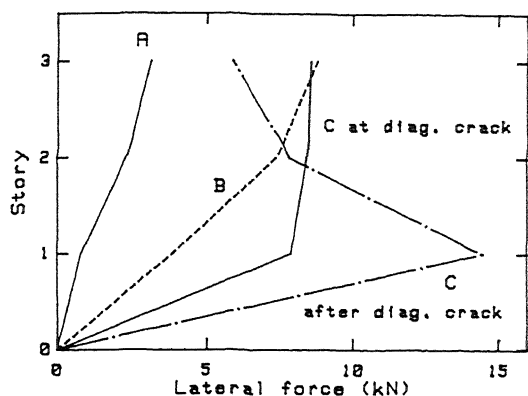


Fig. 7 Lateral force in one wall at the time of maximum base shear force at each run (A, B and C)

ment ratio of 0.1% should be placed in the walls to control the size of the diagonal cracks, avoiding the masonry deterioration (San Bartolomé 1990).

Using such theory, the result would be 7-#5.5 vertical reinforcement for each column; this reinforcement would have controlled the rocking of the specimen around the columns base, preventing its deterioration in a better way than the actual vertical reinforcement. Also, if more horizontal reinforcement would have been provided, it would have controlled the sliding of the upper stories across the first story diagonal cracks produced in run C.

In addition, the following comments can be made:

1. The failure of the specimen was concentrated only at the first story, while at the upper stories the actual shear force never surpassed the theoretical shear strength (VR, formula 1), so their failure was avoided.

2. Referring to the ductility factor which reduces the elastic seismic design force (R_d), the following analysis can be made: if the specimen would have behaved elastically during run C (0.85 g), the total elastic base shear force obtained for run A (0.14 g) would have amplified from 17.3 kN to 105 kN. Then, the value of R_d could be calculated dividing this equivalent elastic shear force by the actual maximum shear force at run C (58 kN, see Figure 8); in this way the ductility factor is $R_d = 105/58 = 1.8$. This value is less than the Peruvian Code specification for confined masonry ($R_d = 2.5$), so the Code does not appear to be conservative.

3. The platform acceleration was 0.54 g at the instant the shear failure occurred. This high value has never been recorded in Perú, so an investigation on the maximum acceleration expected in Perú should be made, because if a masonry building had an adequate wall density it should be able to withstand

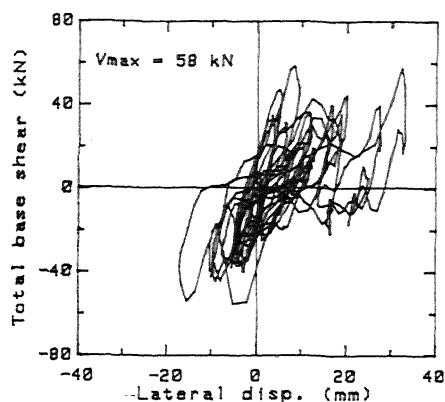


Fig. 8 Total base shear force vs. displacement at level 1 in run C

elastically the earthquakes, without sophisticated designs.

6 CONCLUSIONS

The wall displacements and natural period obtained experimentally in the elastic range, were quite similar with those obtained using a plane frame analysis (transforming the concrete-masonry cross section to masonry). Therefore, a plane frame analysis may be used to obtain the elastic earthquake response of confined masonry buildings.

The research has shown that a shear failure is possible to occur when a strong earthquake hits a confined masonry structure, even in the case that the structure satisfies the ideal characteristics to obtain a flexural failure (slender cantilever, rectangular section, and flexural capacity less than shear capacity). Therefore, the design process of a confined masonry building should include the possibility of a shear type of failure to avoid structural collapse.

A flexural failure would be desirable because it is more ductile than a shear failure; also, the former is more simple to repair. However, more research is needed to obtain this goal.

REFERENCES

- ININVI 1982. Norma peruana de diseño en albañilería E-070.
- Priestley, M.J.N. 1986. Seismic design of concrete masonry shearwalls. ACI Journal, Technical Paper No. 83-8.
- San Bartolomé A. 1990. Albañilería confinada Libro 4 de la colección del ingeniero civil Lima: Colegio de Ingenieros.